ELSEVIER

International Journal of Heat and Fluid Flow 21 (2000) 156–163

International Journal of HEAT AND FLUID FLOW

www.elsevier.com/locate/ijhff

The effect of inclination on the heat transfer between a flat surface and an impinging two-dimensional air jet

Abdlmonem H. Beitelmal [a,*], Michel A. Saad [a], Chandrakant D. Patel [b]

[a] *Department of Mechanical Engineering, Santa Clara University, Santa Clara, CA 95053, USA*
[b] *Hewlett Packard Laboratories, Palo Alto, CA 94304, USA*

Received 18 March 1999; accepted 10 November 1999

Abstract

An experimental study was performed to determine the effect of the inclination of an impinging two-dimensional air jet on the heat transfer from a uniformly heated flat plate. The impingement surface was a stainless steel plate of the same width as the jet nozzle. Local Nusselt numbers were determined as a function of three parameters: (a) inclination angle of the air jet relative to the plate in the range of 90–40°, (b) nozzle exit-to-plate spacing (z/D) in the range of 4–12 and (c) Reynolds number based on the hydraulic diameter of the slot nozzle in the range of 4000–12 000 (corresponding to an exit jet velocity from 6.3 to 18.7 m/s). The results are presented in the form of graphs showing the variation of the local Nusselt number as a function of these parameters. The region of maximum heat transfer shifts towards the uphill side of the plate and the maximum Nusselt number decreases as the inclination angle decreases. The location of the maximum heat transfer region appears to fall between 0 and 3D uphill from the geometrical impingement point, and was found to be insensitive to the Reynolds number in the range used in this study. For low values of inclination angle, the local Nusselt number on the uphill side from the maximum heat transfer point was insensitive to jet exit-to-plate spacing. Correlations are proposed to predict the local Nusselt number as a function of x/D, z/D, θ and Re.

Keywords: Heat transfer; Impinging jet; Jet cooling; Obliquely impinging jet; Inclined jet; Electronics cooling

Notation

a, b	length and width of the cross-sectional dimensions of the slot nozzle (m)
A	surface area (m^2)
D	hydraulic diameter ($= (4ab)/(2a + 2b)$) (m)
h	heat transfer coefficient (W/(m^2 K))
L	length of plate (m)
k_1	thermal conductivity of fiber glass insulation (W/(m K))
k_2	thermal conductivity of Ultem insulation (W/(m K))
k_{air}	thermal conductivity of air (W/(m K))
k	thermal conductivity of the target plate (W/(m K))
Nu	Nusselt number ($= hD/k$)
Q	power dissipation (W)
q''	heat flux (W/m^2)
Re	Reynolds number ($= UD/\nu_{air}$)
T	temperature (°C or K)
U	mean velocity of the air jet at nozzle exit (m/s)
x	distance along the plate measured from the geometrical center (m)
z	vertical distance between the nozzle exit and the center of the plate (m)
ν_{air}	kinematic viscosity (m^2/s)
Δs	displacement of stagnation point (m)
Δx	distance between two adjacent nodes (m)
Δx_1	thickness of fiber glass insulation (m)
Δx_2	thickness of Ultem insulation (m)
θ	angle of inclination relative to nozzle axis (°)
σ	Stefan–Boltzmann constant (5.67×10^{-8} W/(m^2 K^4))
ε	emissivity

Subscripts

c	cross-section
cond	conduction heat transfer
conv	convection heat transfer
j	jet
n	cell number
rad	radiation heat transfer
s	surface
∞	ambient conditions

1. Introduction and background

The thermal control of electronic components is a continuously emerging problem as power loads keep increasing. It is

* Corresponding author.
E-mail addresses: monem@hpl.hp.com (A.H. Beitelmal), cpatel@hpl.hp.com (C.D. Patel).

0142-727X/00/$ - see front matter
PII: S0142-727X(99)00080-6

expected that the power dissipation of future microprocessors will reach 45 W/cm^2 or greater and the electronic industry is eagerly seeking more effective ways to remove localized heat loads.

The design of a thermal control system considers two main requirements; the heat flux to be dissipated and the allowable temperature rise above the local ambient conditions. For heat fluxes below 0.05 W/cm^2 with an allowable temperature difference of about 60°C, radiation and natural convection are usually sufficient means of heat dissipation. For fluxes of 1–2 W/cm^2, a heat transfer coefficient of one order of magnitude higher than that for natural convection is needed and can be achieved by forced convection. For higher heat fluxes, impinging jets provide a potential solution.

In electronic packaging, limitation of space and size creates obstacles in the way of implementing air jets that are normal to the target surface. Inclined jets not only provide localized cooling but also serve to guide the spent air away from the hot spots.

Several papers have been published delineating the increase in Nusselt number due to impinging jets directed normal to the target surface. Martin (1977) and Downs and James (1987) provide extensive reviews of heat and mass transfer using impinging jets. Gauntner et al. (1970) reported that maximum heat transfer occurs at the tip of the potential core of the free jet. The extent of this core is 6–7 nozzle diameters for circular nozzles and is 4–7 slot widths for slot nozzles. Circular nozzles give higher values of heat transfer coefficient whereas slot nozzles give an even distribution of heat and mass transfer. Jambunathan et al. (1992) reviewed published experimental data for the rate of the heat transfer when a circular jet impinges orthogonally on a flat surface for a nozzle exit Reynolds number in the range of 5000–124 000 and for nozzle exit-to-plate surface spacing range from 1.2 to 16. The Nusselt number was expressed in terms of the Reynolds number raised to an exponent which depends on the nozzle exit-to-plate spacing and the distance from the stagnation point. The effect of surface roughness of a heated plate in enhancing the heat transfer between the plate and an impinging air jet was investigated by Beitelman et al. (1997).

A number of studies dealt with investigating the heat transfer between an inclined air jet and a flat surface. McMurray et al. (1966) determined the local heat transfer coefficients of a free surface water jet impinging on a uniformly heated surface at various angles. They proposed correlations for their experimental data in terms of a modified Reynolds number based on the local velocity just outside the boundary layer. Beltaos (1976) studied an obliquely impinging turbulent jet on a flat surface both experimentally and analytically. Measurements of wall pressure were obtained and the stagnation point was identified as the point of maximum pressure on the surface. Semi-empirical methods were used to predict the wall pressure, the wall shear stress and the stagnation point shift due to the jet inclination. Korger and Krizek (1966) used the naphthalene sublimation method to study the heat and mass transfer of an air jet issuing from a slot nozzle and impinging obliquely on a flat plate. Sparrow and Lovell (1980) (see also Lovell, 1978) measured the local mass and heat transfer to an air jet created by an orifice impinging obliquely on a naphthalene test plate. The heat transfer coefficients were determined using the analogy between mass and heat transfer. The angle of inclination varied between 90° and 40°, Reynolds number varied between 2500 and 10 000 and nozzle exit-to-plate distance between 7 and 15. It was shown that inclined jets relocate the stagnation point. This resulted in a reduction of 15–20% of the maximum heat transfer coefficient although the average heat transfer coefficient remained essentially unchanged. Goldstein and Franchett (1988) conducted a study to determine the local heat transfer to a jet issuing from a square-edge orifice and impinging at different angles (90–40°) onto a flat surface. The heat flux was provided by passing an electric current through a thin metallic foil, while the temperature was monitored using the temperature-sensitive liquid crystal technique. The experiments were conducted for nozzle exit-to-plate spacing between 4 and 10 and for Reynolds number between 10 000 and 30 000. The results showed that the displacement of the peak heat transfer location was mainly due to the angle of inclination. A correlation for the local Nusselt number was developed which can be used to determine the average Nusselt number. Garg and Jayaraj (1988) used a finite-difference method to determine the temperature and velocity profiles for a laminar boundary layer generated by an inclined two-dimensional jet over an isothermal surface. Stevens and Webb (1991) investigated the effect of inclination of an axisymmetric liquid jet as it impinges on a flat surface. Their results revealed an uphill shift in the maximum heat transfer point from the geometrical impinging point. The shift distance, normalized by the nozzle diameter, was found to be much less than that of submerged jets for the same angle of inclination. Ward et al. (1991) measured the heat transfer between a circular air jet impinging onto a uniform cross-flow of air over a flat surface coated with naphthalene. Using the sublimation rate of naphthalene along with the Chilton–Colburn analogy, they obtained local heat transfer profiles. The maximum value of heat transfer was found to depend on the impinging jet angle and the velocity ratio between the impinging jet and the cross-flow. Yan and Saniei (1997) investigated the heat transfer from a flat plate to an air jet impinging obliquely from a circular nozzle using the preheated wall transient liquid crystal technique. Angles were varied between 90° and 45° for two Reynolds numbers of 10 000 and 23 000 and for z/D of 4, 7 and 10. Their results showed that the point of maximum heat transfer shifts away from the geometrical impingement point towards the uphill side of the plate. The shift was more pronounced with smaller impinging angles and smaller jet-to-plate spacings.

In the present study, the local heat transfer of an obliquely impinging air jet issuing from a rectangular nozzle is examined. Typical flow regions for such a jet are depicted in Fig. 1. Experiments were performed using a 5.5×50 mm rectangular nozzle with an exit jet velocity ranging between 6.3 and 18.7 m/s. This range of jet velocity is of interest to the cooling problems encountered in the electronic industries. Conventional temperature measurements of the plate surface were used to evaluate the local heat transfer coefficients.

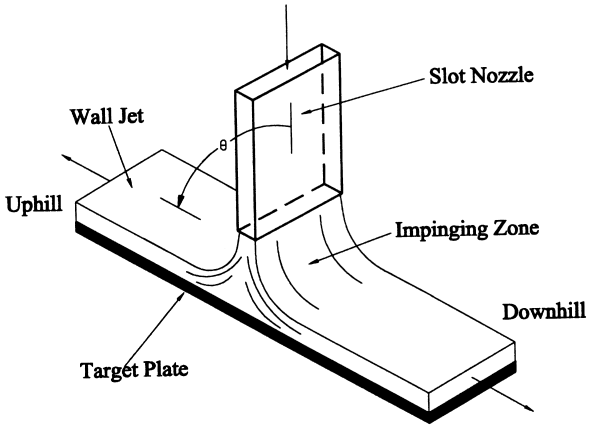

Fig. 1. Flow regions of an inclined impinging jet.

2. Experimental apparatus

A schematic of the experimental apparatus is shown in Fig. 2(a). Compressed air flows through a series of two air filters, an air filter/regulator and then through a flowmeter (Rotameter) into a plenum chamber. A pressure gage connected at the outlet of the flowmeter is used to correct for the flowrate. The plenum chamber shown in Fig. 2(b) is made of plexy-glass and has an inner dimensions of $55 \times 50 \times 25$ mm^3 leading to a straight wall 70 mm long slot nozzle of 5.5×50 mm^2 exit area. A stainless steel plate $200 \times 50 \times 2$ mm^3 was used as a target surface. A patch Kapton heater of less than 0.2 mm thickness, placed at the back of the plate provided a uniform heat flux of 3950 W/m^2. The total power supplied was monitored using two digital multimeters one for the voltage and the other for the current. The target plate and heater were inserted in an insulator/protractor assembly with the top surface of the target plate flushed with the surrounding top surfaces of the insulation. The assembly allowed the tilting of the target plate in increments of 10° from the horizontal position with ±0.2°. Temperatures at the center of the plate (25 mm from each lateral edge) were measured using 11 type T thermocouples inserted through holes of 0.95 mm machined through the thickness of the plate. Electrical discharged machining (EDM) was used to drill the holes and the total material removed was less than 1.3% of the total volume of the target plate. Two layers of material were used to insulate the backside of the target plate and the heater assembly. The first layer was a fiber glass insulation of 3 mm thickness, (thermal conductivity = 0.038 W/(m K)) and the second layer was a GE Ultem of a 50 mm thickness, (thermal conductivity = 0.2 W/(m K)). The instrumentation used to collect the data included multimeters, a DC power supply, Type T thermocouples, an HP 75000B data acquisition unit and an HP Vectra XU 6/200 with an HP Visual Engineering Environment software (VEE).

3. Data reduction

The focus of the present investigation is to examine the effects of the angle of inclination of the jet on the local Nusselt number distribution as a function of $Re, z/D$ and x/D. Experiments were conducted for three different Reynolds numbers of 4000, 7900 and 12 000 (based on the time-averaged flowrate). For each test, the vertical distance between the surface of the plate and the nozzle exit z/D was varied between 4 and 12. Measurements were repeated for inclination angles of 90°, 70°, 60°, 50° and 40° measured from the jet axis, where 90° is the normal-impingement angle.

The heat removal takes place by the three modes of heat transfer: convection, conduction, and radiation. The heat generated by the heater is conducted through the thickness of the plate to the upper surface and eventually is convected by the impinging air jet. The conduction heat loss through the insulation was monitored by measuring the temperature of the insulation and was estimated to be less than 4.1% of the total heat input. An estimate of the heat loss by radiation was also calculated and its maximum was less than 3.3% of the total heat input. Corrections were made for these losses and the convective heat transfer was adjusted accordingly:

$$Q_{\text{conv}} = Q - Q_{\text{cond}} - Q_{\text{rad}}, \tag{1}$$

where Q is the total heat input. Q_{cond} and Q_{rad} are calculated from the following equations:

$$Q_{\text{cond}} = \left[\frac{T_s - T_\infty}{(\Delta x_1/(k_1 A_s)) + (\Delta x_2/(k_2 A_s))} \right] \tag{2}$$

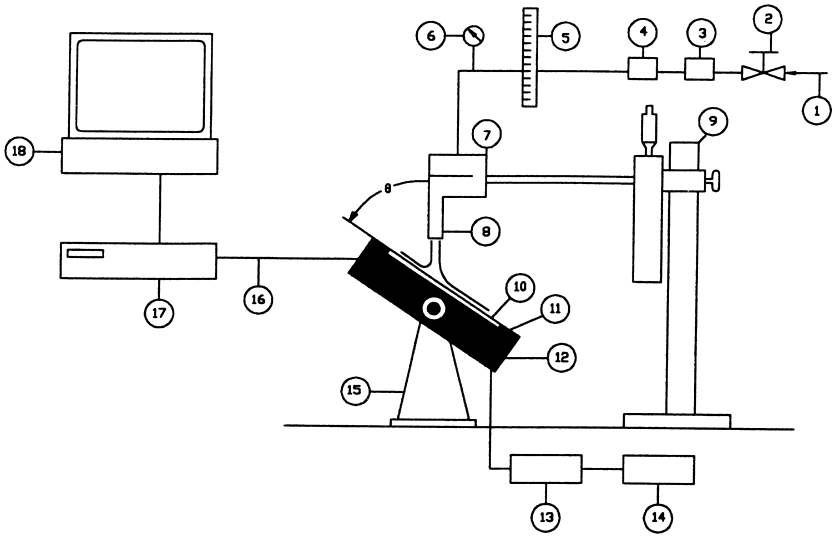

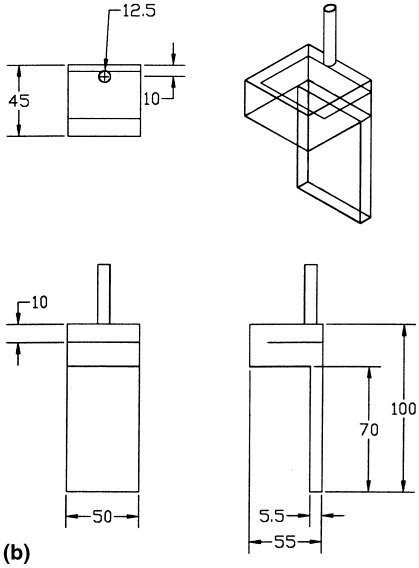

Fig. 2. (a) Schematic of the experimental apparatus; (b) slot nozzle/plenum assembly (dimensions are in millimeters).

and

$$Q_{\text{rad}} = \varepsilon\sigma A_s(T_s^4 - T_\infty^4). \tag{3}$$

Due to the existence of the lateral conduction within the stainless steel, the local heat transfer coefficient was corrected to include this effect. The correction was performed by dividing the plate into 11 cells along the length of the plate (as dictated by the number of the thermocouples used in these experiments) as shown in Fig. 3 and the local heat transfer coefficient at cell n, is calculated from:

$$h = \frac{1}{A_{n,s}(T_n - T_j)}\left[Q_n + \frac{kA_c}{\Delta x}(T_{n+1} - 2T_n + T_{n-1})\right], \tag{4}$$

where A_c is the cross-sectional area between the cells, A_s is the surface area, T_s is the local surface temperature and T_j is the air jet temperature measured at one hydraulic diameter downstream from the slot nozzle exit. Air properties were evaluated at a film temperature of $(T_s + T_j)/2$. The steady-state temperature readings were collected using 11 type T thermocouples. These thermocouples were inserted at the center of the target plate at 15 mm intervals along the length of the plate with one thermocouple located at the central point of the plate.

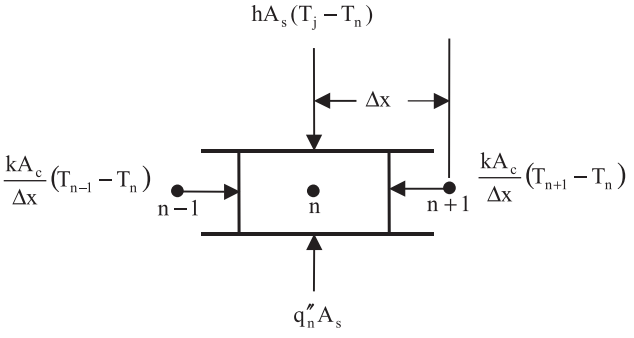

Fig. 3. Numerical approximation of the lateral heat conduction.

A simple finite-difference method was used to validate the numerical accuracy of the local heat transfer coefficient as a function of the number of cells. The relative error was estimated to be less than 1% if the number of nodes were doubled.

The local Nusselt number was determined according to the relation

$$Nu = \frac{hD}{k_{\text{air}}}. \tag{5}$$

4. Results and discussion

An air jet impinging at an angle on a heated flat plate creates an asymmetrical temperature distribution. The temperature of the plate in the downhill direction follows the same trend as in normal impingement with a slight increase in temperature. On the uphill side, the temperature first increases to a maximum and then decreases further uphill. This temperature pattern is attributed to the uneven airflow over the plate where a larger percentage of the air follows the path of least resistance.

In Fig. 4, the local Nusselt number is plotted vs x/D for different values of z/D at constant values of θ and Re, and in Fig. 5, the local Nusselt number is plotted vs x/D for different values of θ at constant values of z/D and Re. These figures are representative samples of the matrix of the total results. For normal impingement the figures show a symmetrical heat transfer distribution around the central point of the target plate. The maximum Nusselt number decreases from its value for normal impingement as the inclination angle decreases with maximum decrease of 15% at $\theta = 40°$ for $Re = 12000$ and $z/D = 4$. For all the values of θ and Re the decrease is less than 11% for $z/D > 4$.

When the plate is tilted (θ decreases), a higher percentage of heat transfer takes place on the downhill side. On the uphill side the local heat transfer first increases in the immediate uphill vicinity of the geometrical impingement point and then

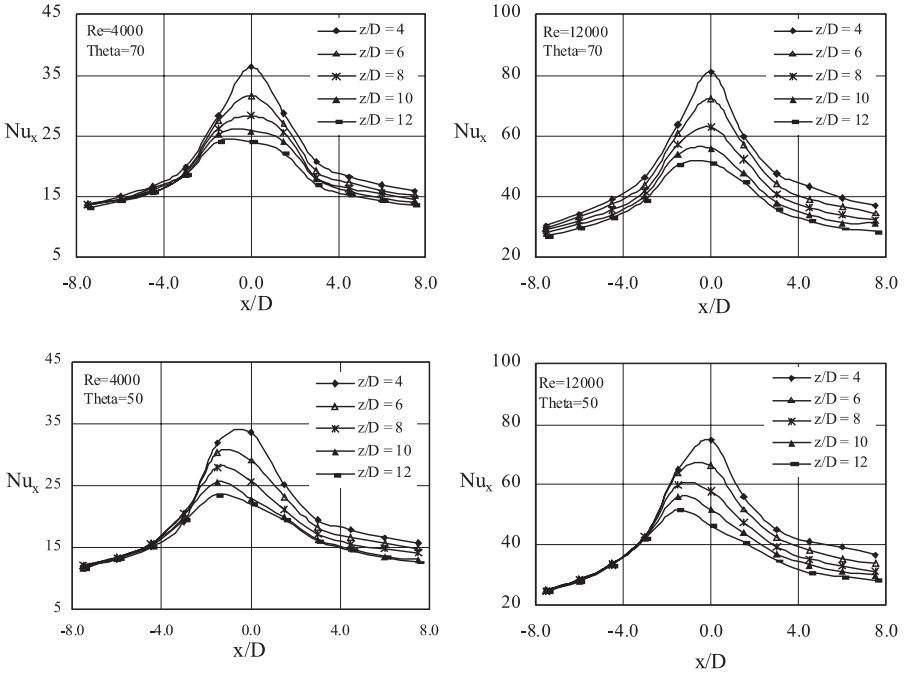

Fig. 4. Local Nusselt number vs x/D for different values of z/D.

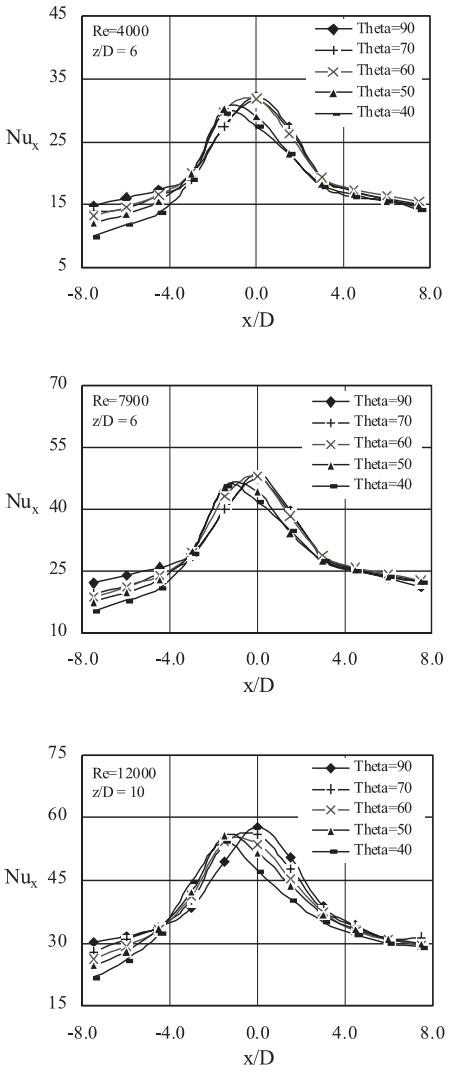

Fig. 5. Local Nusselt number vs x/D for different values of θ.

decreases further uphill. This decrease is attributed to the decrease in momentum of the wall jet. The figures also show a shift in the location of the point of maximum heat transfer (more noticeable for $z/D > 4$) indicating that the shift may depend on the core length of the jet. The Reynolds number affects the heat transfer but it does not appear to affect the shift of the maximum heat transfer point within the range used in this study. Higher Reynolds numbers, however, made the shifting of the maximum heat transfer region easier to detect. This observation agrees with the conclusion reported by Sparrow and Lovell (1980) (see also Lovell, 1978).

In the present study, the location of the displacement of the maximum heat transfer point appeared at $1.5D$ from the geometrical center of the plate. The coarse placement of the thermocouples made it difficult to determine precisely the location of the maximum heat transfer point. However, it is estimated that the displacement of the maximum heat transfer location falls within a distance between 0 and $3D$ from the geometrical impinging point for all values of z/D. Similar findings were reported by Sparrow and Lovell (1980) (see also Lovell, 1978) and by Yan and Saniei (1997). A correlation for the displacement of the point of maximum heat transfer was proposed by Martin (1977) for arbitrary slot widths:

$$\Delta s = 1.4\left[b + 0.11\frac{z}{\sin\theta}\right]. \tag{6}$$

In the present experiments, the shift was calculated based on Eq. (6) and found to vary between 4 mm for $\theta = 70^\circ$ and $z/D = 4$ and 25 mm for $\theta = 40^\circ$ and $z/D = 12$. To develop a relation between the displacement of the maximum heat transfer point and the angle of inclination, it is necessary to collect enough pressure and/or temperature data in the vicinity of the geometrical impinging point at smaller intervals than the ones taken in this study. Pressure measurements and/or temperature-sensitive surface technique similar to the liquid crystals method would give a better resolution to quantify the displacement of the maximum heat transfer point.

Martin (1977) presented the following correlation for the average Nusselt number for normal impingement.

$$\overline{Nu} = \left[\frac{1.53}{\frac{x}{D} + \frac{z}{D} + 1.39}\right] Pr^{0.42} Re^{m}, \quad \begin{cases} 3000 \leqslant Re \leqslant 90\,000, \\ 2 \leqslant z/D \leqslant 10, \\ 2 \leqslant x/D \leqslant 25, \end{cases} \tag{7}$$

where

$$m = 0.695 - \left[\frac{x}{D} + \left(\frac{x}{D}\right)^{1.33} + 3.06\right]^{-1}. \tag{8}$$

The average heat transfer coefficient is given by

$$\bar{h} = \frac{1}{x}\int_0^x h(x)\,\mathrm{d}x, \tag{9}$$

where x is the distance along the plate measured from the impingement point. The average Nusselt number is then calculated from

$$\overline{Nu} = \frac{\bar{h}D}{k_{\text{air}}}. \tag{10}$$

Using the present results, the average Nusselt number for normal impingment was calculated and compared with Martin's correlation. Fig. 6 shows that the correlation matched the present results with a maximum deviation of 19%. This deviation decreased for $z/D > 6$ with 85% of the results fall within 10% of the correlation. The deviation can be attributed to the combined effect of the higher ranges of the Reynolds number and x/D.

McMurray et al. (1966) proposed correlations for a free-surface planar liquid jet data that included a modified Reynolds number based on the local velocity just outside the boundary layer of the wall jet. This allowed them to account for the effects of the distance from the central geometrical point and the vertical distance from the nozzle exit. Correlations were developed for laminar and turbulent wall jets as a function of impingement angle, Prandtl number and the modified Reynolds number. The difference between their correlations and those applicable to a uniform parallel flow over a flat plate was attributed to the difference in the velocity distribution in the impingement region. Their techniques might not be applicable for a submerged jet since the local heat transfer is more sensitive to the vertical distance between the nozzle exit and the surface of the target plate due to entrainment effects. It might also be more practical to correlate the data based on predefined experimental variables than having to measure velocity of the wall jet in order to estimate the local Nusselt number.

In the present study, the local Nusselt numbers were correlated as a function of the four parameters involved z/D, x/D, θ and jet exit Reynolds number. Correlations were developed for three regions: the stagnation region, major axis (downhill region) and minor axis (uphill region). Representative samples of the results are shown in Figs. 7–10.

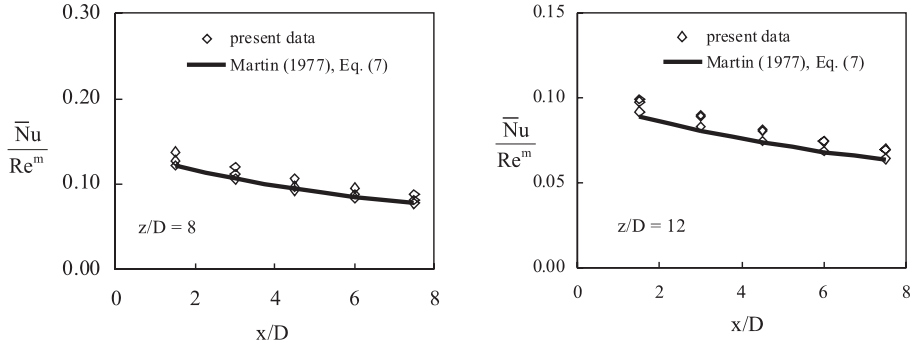

Fig. 6. Comparison of the present results with previous investigations for normal impinging jet (m is given by Eq. (8)).

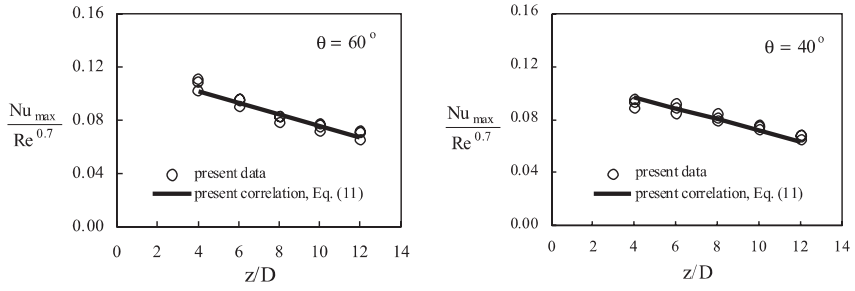

Fig. 7. The maximum Nusselt number correlation for the present data.

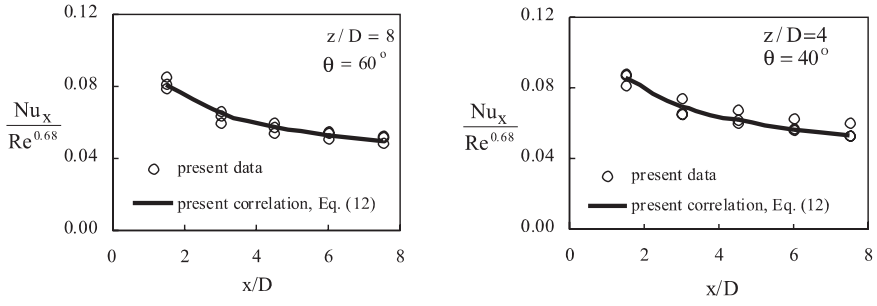

Fig. 8. The Nusselt number correlation for the present data along the major axis.

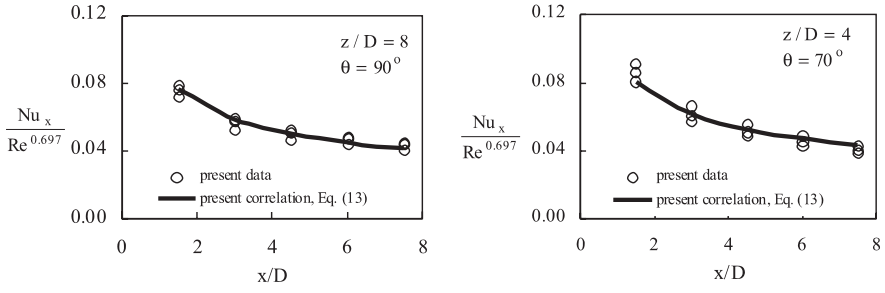

Fig. 9. The Nusselt number correlation for the present data along the minor axis ($70° \leqslant \theta \leqslant 90°$).

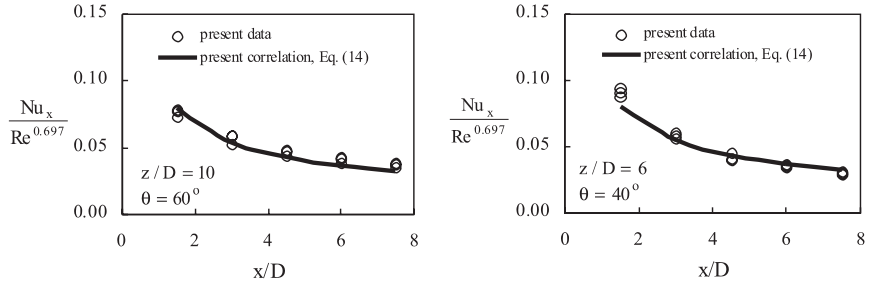

Fig 10. The Nusselt number correlation for the present data along the minor axis ($40^\circ \leqslant \theta \leqslant 60^\circ$).

5. Local Nusselt number correlations

5.1. Impingement region

The flow in this region is quite different from the rest of the wall jet and, as expected, the heat transfer characteristics would also be different. Maximum values of the Nusselt number, obtained from the experimental data, were used to develop the following correlation:

$$Nu_{\max} = 0.09821Re^{0.7}(1.0 + 0.365\sin\theta) \times \left[1.0 - 0.0248\frac{z}{D}\right], \quad \begin{cases} 4000 \leqslant Re \leqslant 12000, \\ 4 \leqslant z/D \leqslant 12, \\ 40^\circ \leqslant \theta \leqslant 90^\circ. \end{cases} \tag{11}$$

The above correlation fits the present data to within 9.0% as shown in Fig. 7.

5.2. Major axis

The local heat transfer data for the major axis (downhill side of the plate) were correlated by the following empirical equation:

$$Nu = 0.0911Re^{0.68}\frac{(1.0 + 0.28\sin\theta)[1.0 - 0.0243(z/D)]}{(x/D)^{0.303}}, \quad \begin{cases} 4000 \leqslant Re \leqslant 12000, \\ 4 \leqslant z/D \leqslant 12, \\ 40^\circ \leqslant \theta \leqslant 90^\circ, \\ 1.5 \leqslant x/D \leqslant 7.5. \end{cases} \tag{12}$$

Eq. (12) fits the present data with a maximum deviation of 13.0% as shown in Fig. 8.

5.3. Minor axis

For the uphill wall jet, it was not possible to correlate the data by a single equation with a reasonable maximum deviation. The data was divided into two sets, one for θ in the range of $70^\circ \leqslant \theta \leqslant 90^\circ$ and the second for $40^\circ \leqslant \theta \leqslant 60^\circ$.

$$Nu = 0.0538\ Re^{0.697}\frac{(1.0 + 0.94\sin\theta)[1.0 - 0.0174(z/D)]}{(x/D)^{0.388}}, \quad \begin{cases} 4000 \leqslant Re \leqslant 12000, \\ 4 \leqslant z/D \leqslant 12, \\ 70^\circ \leqslant \theta \leqslant 90^\circ, \\ 1.5 \leqslant x/D \leqslant 7.5. \end{cases} \tag{13}$$

The above equation fits the present data in the range specified for θ with a maximum deviation of less than 11.5% as shown in Fig. 9.

$$Nu = 0.103Re^{0.697}\frac{(1.0 + 0.0633\sin\theta)[1.0 - 0.0079(z/D)]}{(x/D)^{0.558}}, \quad \begin{cases} 4000 \leqslant Re \leqslant 12000, \\ 4 \leqslant z/D \leqslant 12, \\ 40^\circ \leqslant \theta \leqslant 60^\circ, \\ 1.5 \leqslant x/D \leqslant 7.5. \end{cases} \tag{14}$$

The above correlation fits the present data within 17% as shown in Fig. 10.

Eqs. (13) and (14) show that the dependency of $Nu/Re^{0.697}$ on z/D decreases while the dependency on x/D increases as the inclination increases. Note that in the proposed correlation equations the exponent of Re varies between 0.68 and 0.70 which indicate its dependency on the geometrical location.

Based on the standard uncertainty analysis, Moffat (1988), the steady-state uncertainties of the collected data and calculated parameters were evaluated. The uncertainty in temperature measurements was ± 0.5°C, in the flowrate it was less than 4.2%, in the electric power it was less than 1.3%, in the Reynolds number it was about 5% and it was less than 4.1% in the Nusselt number.

6. Conclusions

(1) Local Nusselt numbers were experimentally determined for a two-dimensional air jet impinging obliquely on a uniformly heated flat surface. The measured data was in the range of $4000 \leqslant Re \leqslant 12000$, $4 \leqslant z/D \leqslant 12$ and $40^\circ \leqslant \theta \leqslant 90^\circ$. Plotted results of the local Nusselt number are presented as a function of Re, θ, z/D and x/D.

(2) The distribution of the local Nusselt number moves away from symmetry as the inclination angle decreases. The distributions for different values of z/D tend to coalesce on the uphill side of the target surface beyond the maximum heat transfer point and diverge slightly on the downhill side of the plate. This means that the heat transfer distribution becomes less sensitive to the jet exit-to-plate spacing on the uphill side of the plate.

(3) The shift of the maximum heat transfer point moves towards the uphill side of the plate. This is due to the change in the magnitude and direction of the velocity of the air jet. The displacement depends on the angle of inclination and the vertical distance between the plate and the nozzle exit. It was found to be insensitive to the Reynolds number for the range used in this study.

(4) Although detailed measurements of the displacement of the maximum heat transfer point were not made, it maybe stated, based on the present results that the displacement falls between 0 and $3D$ away from the geometrical impinging point.

(5) Correlations for the local Nusselt number are proposed for three regions of the target surface: impingement region, major axis and the minor axis.

Acknowledgements

The authors would like to acknowledge the support for this work in terms of equipment grant from Gene Emerson and Al Barber of the STD at Hewlett Packard Laboratories and wish to thank them for their help and encouragement.

References

Beitelmal, A.H., Saad, M.A., Patel, C.D., 1997. Heat transfer of an air jet impinging on a rough surface. In: ASME National Heat Transfer Conference, HTD-vol. 347, Baltimore, Maryland.

Beltaos, S., 1976. Oblique impingement of circular turbulent jets. J. Hydraulic Res. 14, 17–36.

Downs, S.J., James, E.H., 1987. Jet impingement heat transfer – a literature survey. In: ASME National Heat Transfer Conference, ASME 87-HT-35, Pittsburgh, PA.

Garg, V.K., Jayaraj, S., 1988. Boundary layer analysis for two dimensional slot jet impingement on inclined plates. J. Heat Transfer 110, 577–582.

Gauntner, J., Livingood, N.B., Hrycak, P., 1970. Survey of literature on flow characteristics of a single turbulent jet impinging on a flat plate, NASA TN D-5652, Lewis Research Center.

Goldstein, R.J., Franchett, M.E., 1988. Heat transfer from a flat surface to an oblique impinging jet. J. Heat Transfer 110, 84–90.

Jambunathan, K., Lai, E., Moss, M.A., Button, B.L., 1992. A review of heat transfer data for single circular jet impingement. Int. J. Heat Fluid Flow 13, 106–115.

Korger, M., Krizek, F., 1966. Mass transfer coefficient in impingement flow from slotted nozzles. Int. J. Heat Mass Transfer 9, 337–344.

Lovell, B.J., 1978. Local transfer coefficients for impingement of an axisymmetric jet on an inclined flat plate. M.S. Thesis, Mechanical Engineering Department, University of Minnesota, MN.

Martin, H., 1977. Heat and mass transfer between impinging gas jets and solid surfaces. Adv. Heat Transfer 13, 1–60.

McMurray, D.C., Myers, P.S., Uyehara, O.A., 1996, Influence of impinging jet variables on local heat transfer coefficients along a flat surface with constant heat flux. In: Proceedings of the Third International Heat Transfer Conference, vol. 2, Chicago, IL, pp. 292–299.

Moffat, R.J., 1988. Describing the uncertainties in experimental results. J. Fluid Sci. 1, 3–17.

Sparrow, E.M., Lovell, B.J., 1980. Heat transfer characteristics of an oblique impinging circular jet. J. Heat Transfer 102, 202–209.

Stevens, J., Webb, B.W., 1991. The effect of inclination on local heat transfer under an axisymmetric free liquid jet. Int. J. Heat Mass Transfer 34, 1227–1236.

Ward, J., Oladiran, M.T., Hammond, G.P., 1991. Effect of nozzle inclination on jet-impingement heat transfer in a confined cross-flow. ASME, 91-HTD-vol. 181, pp. 25–31.

Yan, X., Saniei, N., 1997. Heat transfer from an oblique impinging air jet to a flat plate. Int. J. Heat Fluid Flow 8 (6), 591–599.